Acta Mechatronica - International Scientific Journal about Mechatronics
Volume: 5 2020 Issue: 4 Pages: 47-52 ISSN 2453-7306

doi:10.22306/am.v5i4.68

Received: 05 Oct. 2020
Revised: 30 Oct. 2020
Accepted: 09 Nov. 2020

APPLICATION OF DENAVIT HARTENBERG METHOD IN SERVICE ROBOTICS

Erik Prada
Technical University of Kosice, Faculty of Mechanical Engineering, Letna 9, Kosice, Slovak Republic, EU, erik.prada@tuke.sk (corresponding author)
Srikanth Murali
Technical University of Kosice, Faculty of Mechanical Engineering, Letna 9, Kosice, Slovak Republic, EU, srikanth.murali@tuke.sk
Ľubica Miková
Technical University of Kosice, Faculty of Mechanical Engineering, Letna 9, Kosice, Slovak Republic, EU, lubica.mikova@tuke.sk
Jana Ligušová
KYBERNETES, s.r.o., Omska 14, Kosice, Slovak Republic, EU, jana.ligusova@kybernetes.sk

Keywords: Kinematics, Denavit-Hartenberg method, Service Robot
Abstract: This work focuses primarily on the D-H method, as one of the most important methods used in the process of designing robotic structures. In the introduction, the history of the D-H method and its general use is briefly mentioned. In the following section, the algorithm for applying D-H in the form of mathematical formalism is explained. In this part, the individual steps of creating transformational relationships are explained in more detail. The next chapters deal in more detail with individual application types within service robotics. The first type deals with the application deployment of the mobile robotic platform, the second deals with the mobile humanoid robotic structure, the other deals with the four-legged robotic mechanism and the last type with the application of the robotic arm.

1 Introduction

With the fast advancement of robot innovation, service robots are slowly showing up in a wide area to the public. Service robots are the one which will perform work in a fully automatic or semi-automatic way for a human or another equipment for which the service robot is made for. Scientific researchers from various parts of the globe are investing their time and effort towards the control and intelligent algorithm of the service robots. One of the important elements of a service robot is its arm also known as the manipulator [1]. It is a significant characteristic of the service robot to have a flexible arm which has to be controlled as per its requirement [2]. Kinematics is the area where the control of the arm is designed to serve its purpose and analyse the arm movement to be effective according to the mechanical structure of the robot.

The robot manipulator is classified according to the kinematic structure as serial, parallel and hybrid manipulator. In serial manipulator, each individual link is connected to other link in series by different joints, usually prismatic or revolute joints. It is also called open loop chain. Parallel manipulator on the other hand consists of several closed loop chains where one joint in the chain is actuated and the other joints are passive. A hybrid manipulator combines the serial and parallel manipulator. The above image (Figure 1) shows the classification of manipulator according to their kinematic structure. We are interested towards the serial manipulator in this document and we will dive deep into it. As mentioned previously, the serial manipulator comprises of several links connected in series. One end of the arm is attached to the ground and the other end of the arm is made to move freely in space. The fixed arm is known as base and in the free end a mechanical hand or gripper is attached. The important aspect for a robot to perform its task is the establishment of the location of end effector relative to its base. This method of establishing the location offend effector with respect to the base is known as position analysis problem. There are two subdivision for solving the position analysis problem. One is direct position method or direct kinematics method. In this method, the goal is to find the location of the end effector in which the joint variables are given. The other is the inverse position or inverse kinematics method in which the location of end effector is known, and the aim is to find the joint variables that are needed to bring the manipulator to its required position [3-6].

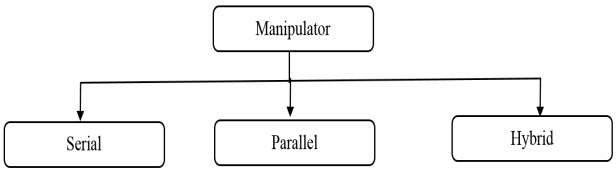

Figure 1 Classification of Manipulator according to kinematic structure

Acta Mechatronica - International Scientific Journal about Mechatronics
Volume: 5 2020 Issue: 4 Pages: 47-52 ISSN 2453-7306

APPLICATION OF DENAVIT HARTENBERG METHOD IN SERVICE ROBOTICS

Erik Prada; Srikanth Murali; Ľubica Miková; Jana Ligušová

There are many methods available to deal with the Kinematics of the manipulator. The best among the available method has to be chosen with due to the robot's mechanical structure. Most successful and widely used methods include numerical method, geometry method, optimization algorithm and the vector algebra method. The numerical method refers mainly to the Denavit-Hartenberg method [7]. It is also called as 4x4 matrix method or simply D-H method. Jacques Denavit and Richard Hartenberg in 1955 introduced this method in order to standardize the coordinate frames for spatial linkages. This method is a consistent and short description depicting the kinematic relations among the links connected by 1 degree-of-freedom lower pair joints, usually, rotational and prismatic joints. Nowadays, various other methods were introduced by this method still shows to be efficient for several specific movements of the robotic manipulator. We will be looking into this method and then some of the areas where this method is used in positioning the robotic manipulator in achieving their requirements [8-10].

2 Denavit Hartenberg Method

In this method, the coordinate frames are attached to the joints between two links such that one of the transformations is associated with the joint [Z], while the second is associated with the link [X]. For a serial robot consisting of n links, the coordinate transformations from the kinematic equations of the robot are given by (1),

$$[T] = [Z_1][X_1][Z_2][X_2] \dots [Z_{n-1}][X_{n-1}][Z_n][X_n] \qquad (1)$$

where [T] denotes the transformation locating the end-link. Below is an image showing the four parameters involved in the D-H convention.

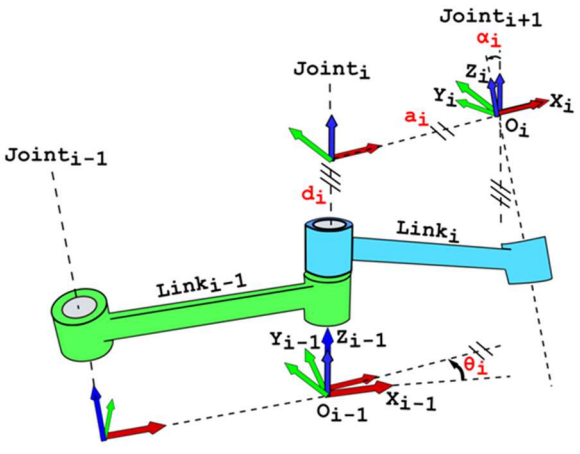

Figure 2 Four parameters of D-H convention [7]

From the above image we can depict that the four parameters associated with the D-H convention which are represented in red colour. They are θ_i, d_i, a_i, α_i. Using these four parameters we can translate the coordinates from O_{i-1}, X_{i-1}, Y_{i-1}, Z_{i-1} to O_i, X_i, Y_i, Z_i. These four parameters are known as D-H parameters and below is the process for achieving the transformations. The variables denote the following:

- d, offset along the previous Z axis to the common normal,
- θ, angle from previous Z, from old X to new X,
- a, length of the common normal (also denoted as r). Assuming revolute joint, this is the radius about previous Z,
- α, angle about common normal, from old Z axis to new Z axis.

The D-H parameters gives a standard way to write the manipulator's kinematic equation, especially for serial manipulators. This can be done by using a matrix (2) to express the position and orientation of one body with respect to another body.

$$^{n-1}T_n = \begin{bmatrix} \cos\theta_n & -\sin\theta_n\cos\alpha_n & \sin\theta_n\sin\alpha_n & a_n\cos\theta_n \\ \sin\theta_n & \cos\theta_n\cos\alpha_n & -\cos\theta_n\sin\alpha_n & a_n\sin\theta_n \\ 0 & \sin\alpha_n & \cos\alpha_n & d_n \\ 0 & 0 & 0 & 1 \end{bmatrix} \qquad (2)$$

This can be written as (3):

$$^{n-1}T_n = \begin{bmatrix} R & T \\ 0\ 0\ 0 & 1 \end{bmatrix} \qquad (3)$$

where: R is the 3x3 matrix representing the rotation and T is 3x1 matrix representing translation.

2.1 *Advantages of D-H method*

Some of the advantages of the D-H convention are as follows:

- Main aspect of D-H convention is the roto-translation in terms of only 4 variables for each individual link when compared with the canonical form involving 6 variables (3 for translation and 3 for rotation).
- It is very easy and convenient to get the transformation of number of links attached in series by multiplying the transformation series rather than calculating manually by basic geometry method [11-12].
- Faster convergence of estimated states is achieved in a least-squares technique by employing D-H parameters to it. Simply saying, this will help in the reduction of error faster [11-12].
- D-H parameters are more consistent and simpler when compared to Product of Exponential (POE) parameters with respect to serial link robots [13].
- Minimal representation is achieved with D-H parameters. It is nice when worked with linear algebra computations.
- D-H based algorithm model acts as an efficient tool for sub-problems and also for real-time inverse kinematics solution for the trajectory of serial link robots [2].

Acta Mechatronica - International Scientific Journal about Mechatronics
Volume: 5 2020 Issue: 4 Pages: 47-52 ISSN 2453-7306

APPLICATION OF DENAVIT HARTENBERG METHOD IN SERVICE ROBOTICS

Erik Prada; Srikanth Murali; Ľubica Miková; Jana Ligušová

3 Applications of D-H Method

3.1 Body Activity Interaction for a Service Robot

In the field of intelligent robots, the interaction with human body plays a major role. Body Activity Interaction in a service robot [13] works in a way to realize the body activities and interact accordingly. Microsoft Kinect is utilized to capture the body movements and the action recognition module provides input signals depending on the captured movements programmed into it. The field data from Kinect is capable of tracking the 20 bones of human body and by processing this data we can obtain the recognition action for the robot movement. Some of the field data includes tracking the human shoulder, wrist joints, elbows, etc. Below image (Figure 3a) shows the robot's structure and the motion control of the robotic manipulator (Figure 3b). The Kinematic model consists of 6 degree of freedom right arm of the robot consisting of the links and it is solved with the help of D-H convention. The parameters used for solving the D-H convention are listed in the table (Table 1).

From the table, we can depict that, the θ_i is the i-1th joint angle and α_i is the i-th torque angle. Whereas the offset link is denoted as di and ai is the length of the link. MATLAB Robotics Toolbox is used to control the kinematics motion planning of the robotic arm which are used to design the hand shaking and hand waving motions. Figure 4 shows the planning of the variations in joint angle for performing the handshaking motion computed in MATLAB [13].

Table 1 Denavit-Hartenberg parameters for the robotic manipulator [13]

i	θ_i	α_i	a_i (m)	d_i (m)
x1	θ_1	-90º	0	0.065
2	θ_2 - 90º	-90º	0	0
3	θ_3 + 90º	90º	0	0.170
4	θ_4	-90º	0	0
5	θ_5 - 90º	90º	0	0.169
6	θ_6 + 90º	0º	0	0

Figure 3 a) Structure of the robot [13]

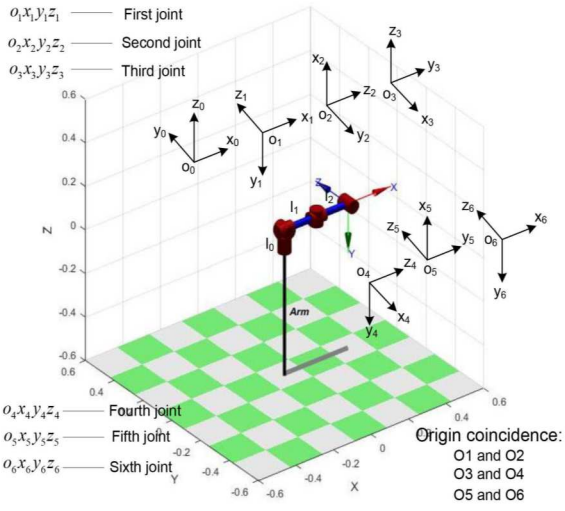

Figure 3 b) Motion control of the arm [13]

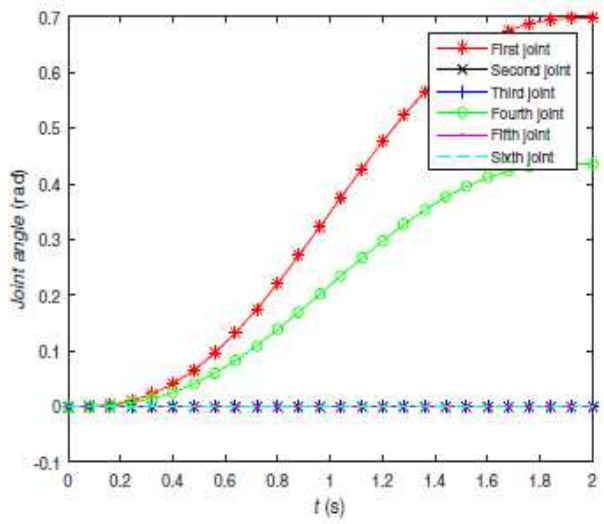

Figure 4 a) Right arm lifting [13]

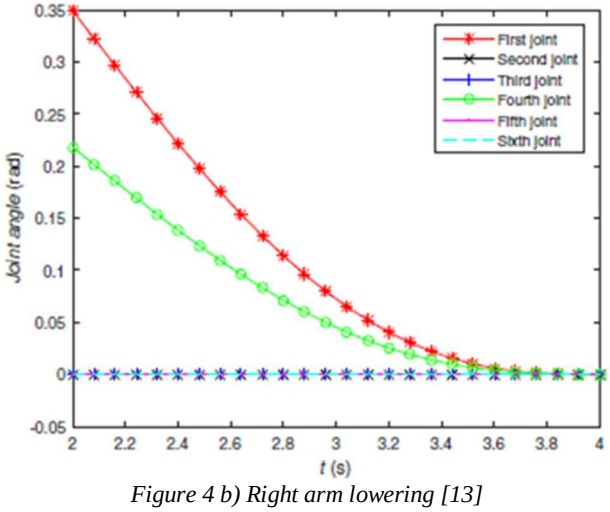

Figure 4 b) Right arm lowering [13]

Acta Mechatronica - International Scientific Journal about Mechatronics
Volume: 5 2020 Issue: 4 Pages: 47-52 ISSN 2453-7306

APPLICATION OF DENAVIT HARTENBERG METHOD IN SERVICE ROBOTICS

Erik Prada; Srikanth Murali; Ľubica Miková; Jana Ligušová

From the above images we can derive that the positive values are obtained for the first and the fourth joint meaning that rotation about fixed degrees in fixed direction of the shoulder and elbow joints thus extending the right arm. For lowering the right arm, the first and fourth joint are taking the negative values [13].

3.2 Mobile Humanoid Robot

Mobile humanoid robot [14] has been invented to assist elderly people. The robot is constructed with a visual sensor for recognizing objects. At the lower part of the robot is placed the Laser Range Finder which helps to detect obstacles. Once the object is identified, the robot moves toward it and then it uses the grasping motion to hold the object. It can also be used in hospitals or homes to work actively with the humans in real environment. Below image (Figure 5a) shows the robot design and the image (Figure 5b) represents the kinematic mechanism of the robot manipulator.

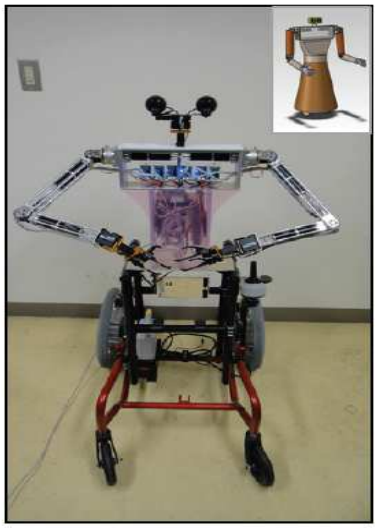

Figure 5 a) Showing the mechanical design of mobile Humanoid robot [14]

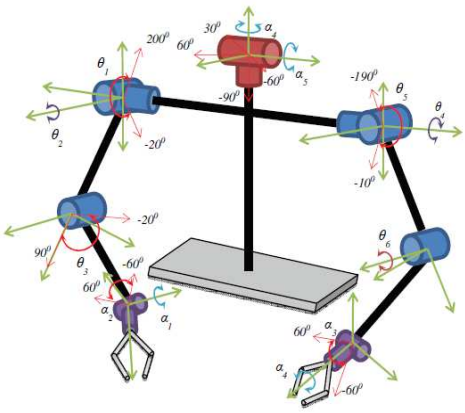

Figure 5 b) Showing the kinematics structure of mobile Humanoid robot [14]

Table 2 Denavit-Hartenberg parameters for the mobile service robot [14]

Joint, i	α_i	a_i	d_i	θ_i
0A	90°	0	d_1	θ_1
B	0	a_1	0	θ_2
C	0	a_2	0	θ_3
D	0	0	0	Gripper

The table (Table 2) shows the D-H parameter used in solving the kinematics of the robot and the matrix (4) representation of the D-H convention is given as follows:

$$T_4^0 = \begin{bmatrix} c_1\,c_{23} & -c_1\,s_{23} & s_1 & c_1(a_3\,c_{23} + a_2\,c_2) \\ s_1\,c_{23} & -s_1\,s_{23} & -c_1 & c_1(a_3\,c_{23} + a_2\,c_2) \\ s_{23} & c_{23} & 0 & a_3\,s_{23} + a_2\,s_2 + d_1 \\ 0 & 0 & 0 & 1 \end{bmatrix} \quad (4)$$

From the D-H Matrix we can derive that the orientation of the end effector was represented by the first three columns and the position of the end effector is represented by the last column such that, in terms of joint angles we can derive both the position and orientation of the end effector [14].

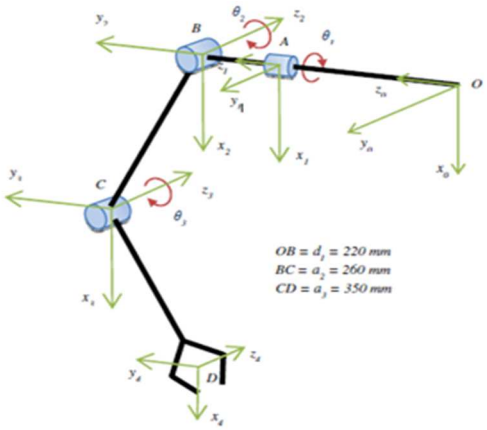

Figure 6 Manipulator for D-H convention [14]

3.3 Quadruped robot

Quadruped [15] robots are used to mimic the animal waling gait. It has four legs instead of wheels. The main advantage is that they can be used to walk on terrain and extremely hard surfaces. This is the main difference among the quadrupeds when compared with that of the wheeled vehicles where the vehicles with wheel will be stuck in place of the obstacles on a rough path and the quadrupeds can easily move pass the obstacles by adjusting their height. The D-H convention is used for deriving the kinematic solutions and thus these solutions can be used for simulating the movement using 3D software. The robot can be controlled via an Android application using the Bluetooth Technology. The robot hosts six types of movements: forward, backward, left walking, right walking, rotation in clockwise and anti-clockwise

APPLICATION OF DENAVIT HARTENBERG METHOD IN SERVICE ROBOTICS
Erik Prada; Srikanth Murali; Ľubica Miková; Jana Ligušová

direction. Obstacles within the range of 300 cm are identified with the help of ultrasound sensors. The robot is capable of moving in parallel towards an identified obstacle in a way to avoid colliding with it. Each of the four legs of the quadruped has 2 degrees of freedom which resembles the hip and knee joints of the leg and in total it has 8 degrees of freedom. In this case, the following are the D-H parameters associated with the quadruped movement: the link length is represented as a and the link twist as A. The link offset as and the angle of joint as T. Below is the D-H parameters table (Table 3) and the matrix (5) representing the D-H convention [15].

Table 3 D-H parameters for quadruped robot [15]

Link	a	A	d	T
L_1	a_1	90	0	t_1
L_2	a_2	0	0	t_2

$$T = \begin{bmatrix} c_1c_2 & -c_1s_2 & s_1 & c_1(a_1 + a_2c_2) \\ s_1c_2 & -s_1s_2 & -c_1 & s_1(a_1 + a_2c_2) \\ s_2 & c_2 & 0 & a_2s_2 \\ 0 & 0 & 0 & 1 \end{bmatrix} \quad (5)$$

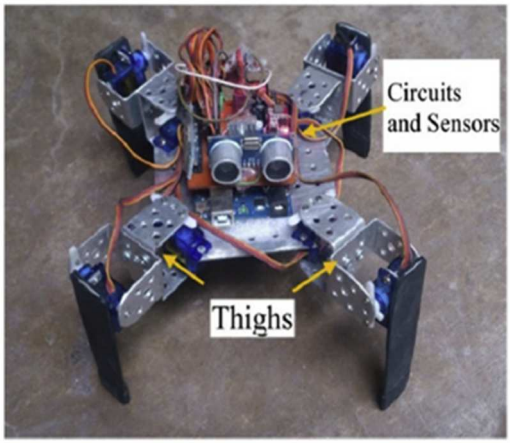

Figure 7 a) Quadruped robot - top view [15]

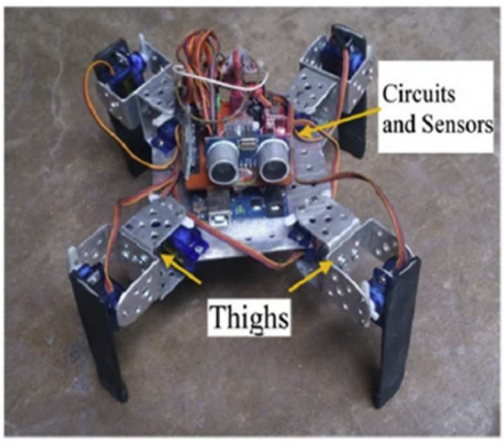

Figure 7 b) Quadruped robot – front view [15]

3.4 Robotic Arm

The robotic arm [16] here discussed is used for pick and place operations. The robot is provided with the voice recognition and image processing capabilities. The simulation of the mechanical structure in forward kinematics is carried out in MATLAB and the design is using the Denavit-Hartenberg convention. The serial link manipulator is achieved by the connection of the links with the joints in a sequential manner and thus it is analysed with the D-H parameter method. By this, we can obtain the result in a matrix where the Cartesian position of the end effector is expressed in terms of the joint coordinates. The D-H parameter is shown in the table (Table 4).

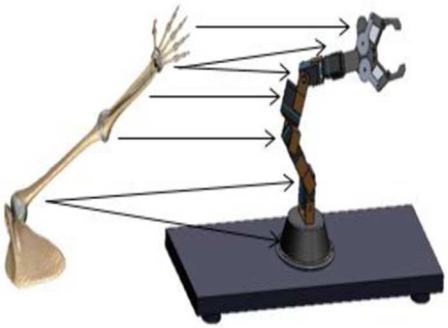

Figure 8 a) Design of the robot arm [16]

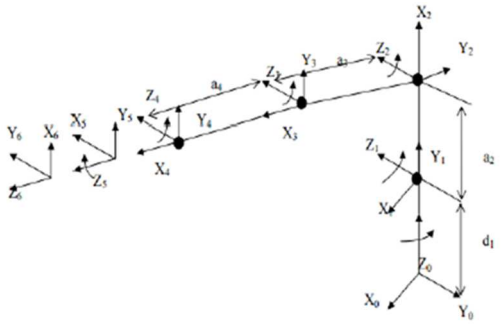

Figure 8 b) Kinematic analysis of the arm [16]

Table 4 D-H parameters of robot arm [16]

Joint, i	α_{i-1}	d_i	θ_i	a_{i-1}
1	90°	d_1	θ_1	0
2	0°	0	θ_2	a_2
3	0°	0	θ_3	a_3
4	90°	0	θ_4	a_4
5	90°	0	θ_5	0
6	0°	d_6	θ_6	0

The arm of the robot is constructed in resemblance to the human arm joints like shoulder, elbow and wrist. Each of the elbow joints has a single degree of freedom and the wrist can project in two planes namely, Rolland pitch, as a result of providing more flexibility for the end effector in terms of manipulation of the object [16].

4 Conclusions

The Denavit-Hartenberg method is one of the effective and simple way to derive the kinematics of a robot mechanism. There are a number of applications apart from the topics discussed in this document that involves the use of Denavit-Hartenberg conventions. Even though, a number of methods are available, the D-H method is still one of the widely used method to solve the kinematics problem in a robot.

Acknowledgement

The authors would like to thank to Slovak Grant Agency project VEGA 1/0389/18, grant project KEGA 018 TUKE-4/2018, grant project KEGA 030 TUKE-4/2020 supported by the Ministry of education of Slovak Republic. This paper was published in cooperation with company KYBERNETES s.r.o. within the project "Research and development of the ECOGI product at KYBERNETES", ITMS Code of Project: 313012Q955.

References

[1] Automation, LJ Welding, Welding Manipulators Subarc Welding & CMT Manipulators: [Online], Available: www.ljwelding.com [21 Sep 2020], 2020.

[2] TSAI, L.W.:.*Robot Analysis: The Mechanics of Serial and Parallel Manipulators*, John Wiley sons, 1993.

[3] GMITERKO, A., KELEMEN, M., DOVICA, M., CAPÁK, M.: *Miniature mobile robot for moving in a tube with small diameter*, Proceedings of the 2nd International Conference Mechatronics and Robotics '99, Brno, Czech Republic, pp. 67-70, 1999.

[4] VITKO, A., JURIŠICA, L., BABINEC, A., DUCHOŇ, F., KĽÚČIK, M.: *Some Didactic Problems of Teaching Robotics*, Proceedings of the 1st International Conference Robotics in Education 2010, Bratislava, Slovak University of Technology in Bratislava, pp. 27-30, pp. 67-70, 2010.

[5] HAVLÍK, Š., HRICKO, J., PRADA, E., JEZNÝ, J.: *Linear motion mechanisms for fine position adjustment of heavy weight platforms*, International Conference on Robotics in Alpe-Adria Danube Region RAAD 2019, Advances in Service and Industrial Robotics, pp 19-25, 2020.

[6] VIRGALA, I., KELEMEN, M., PRADA, E., LIPTÁK, T.: Positioning of Pneumatic Actuator Using Open-Loop System, *Applied Mechanics and Materials*, Vol. 816, pp. 160-164, 2015.

[7] SPONG, M.W., VIDYASAGAR, M.: *Robot Dynamics and Control*, New York: John Wiley & Sons, 1989.

[8] PRADA, E., BALOČKOVÁ, L., VALÁŠEK, M.: Elimination of the Collision States of the Effectors of Industrial Robots by Application of Neural Networks, *Applied Mechanics and Materials*, Vol. 798, pp. 276-281, 2015.

[9] PRADA, E., MIKOVÁ, Ľ., SUROVEC, R., KENDEROVÁ, M.: *Complex kinematic model of snake-like robot with holonomic constraints*, Technológia Europea 2012: sborník příspěvků mezinárodní vědecké konference k problematice technologických a inovačních procesů : ročník 2 : 11.-14. prosince 2012, Hradec Králové, Česká republika. - Hradec Králové : MAGNANIMITAS, 2012, pp. 81-87, 2012.

[10] MENDA, F., ŠARGA, P., PRADA, E., TREBUŇA, F.: *SolidWorks API for Ring-Core simulations*, 2014 IEEE 12th International Symposium on Applied Machine Intelligence and Informatics (SAMI), Herl'any, 2014, pp. 151-155, 2014. doi:10.1109/SAMI.2014.6822397.

[11] HE, R., ZHAO, Y., YANG, S., YANG, S.: Kinematic-Parameter Identification for Serial-Robot Calibration Based on POE Formula, *Robotics, IEEE Transactions on*, Vol. 26, No. 3, pp. 411-423, 2010.

[12] HAYATI, S.A.: *Robot arm geometric link parameter estimation*, Decision and Control, 1983. The 22nd IEEE Conference on, pp. 1477-1483, December, 1983.

[13] WU, L., CRAWFORD, R., ROBERTS, J.: *An Analytic Approach to Converting POE Parameters into D-H Parameters for Serial-Link Robots*, *IEEE ROBOTICS AND AUTOMATION LETTERS*, Vol. 2, No. 4, pp. 2174-2179, 2017.

[14] ZULKIFLI, M., GENCI, C.: *Development of a New Mobile Humanoid Robot for Assisting Elderly People*, Procedia Engineering, Volume 41, pp. 345-351, 2012. doi:10.1016/j.proeng.2012.07.183

[15] MOIN, U.A., RAFIQUL, I.S., ATIQUR, R.A.: Development of an 8DOF quadruped robot and implementation of Inverse Kinematics using Denavit-Hartenberg convention, *Heliyon*, Vol. 4, No. 12, pp. 2-19, 2018, doi:10.1016/j.heliyon.2018.e01053

[16] PATHIRANA, M.G.K., PERARA, K.T.K., SIRITHUNGE, Ch., JAYASEKARA, B., SRIMAL, A.: *Design and Simulation of a Robotic Arm for a Service Robot*, EECon, 2015.

Acta Mechatronica - International Scientific Journal about Mechatronics
Volume: 5 2020 Issue: 4 Pages: 53-60 ISSN 2453-7306

doi:10.22306/am.v5i4.69

Received: 19 Oct. 2020
Revised: 21 Nov. 2020
Accepted: 14 Dec. 2020

DESIGN AND FABRICATION OF RUNNING CHEETAH MECHANICAL TOY USING FOUR-BAR LINKAGE

Adimas Wicaksana
Universitas Pamulang, Jl. Surya Kencana no. 1 Pamulang, dosen01678@unpam.ac.id

Keywords: four-bar linkage, mechanism design, 3D printing
Abstract: Four-bar is the simplest planar 1-DOF closed loop linkage. It has been studied for centuries for its versatility and simplicity. In this paper a novel design method to obtain a four-bar linkage given a path and its endpoints will be presented. This method will then be applied to a case study of making a model that produces a specified movement based on reference animation. The mechanism obtained had an average root-mean-square of position error of roughly 14.3 pixels for front leg and 25.9 pixels for hind leg. This number is quite small compared to the perimeter of the traced path, which are 530 pixels and 617 pixels for front leg and hind leg respectively. A prototype model of the designed mechanism was fabricated to verify its manufacturing viability and to confirm the correctness of the path generated.

1 Introduction

There has been quite a considerable interest in development of motion guided toy following the publication of a seminal work by Zhu et al [1]. Recent developments include T-Rex, Pushing Man and Dog toy [2], Bull toy and Dancing Lantern [3], and Dancing Automaton [4] from motion capture sequence. However, the commonality between the designs of all these toys is that they are machine elements that are relatively difficult to produce like gears and cams. These elements would require motion in at least two axes to be produced correctly. This would mean that one would require a CNC machine to produce the mechanism. One solution to simplify the mechanism would be to use one of the simplest planar mechanism, which is a four-bar linkage. Unfortunately, most of the case study for four-bar design has been focusing mostly on straight lines [5], circle [6], and figure-eight-like motions [7]. Most of the current work also seems to focus on Evolutionary Algorithm/Genetic Algorithm whose emphasis is on letting the computer attempt optimize four-bar parameter by itself without any additional heuristic from human [8,9] however the effectiveness of these techniques depends highly on initial position chosen. There is no guarantee that there will be convergence during solution space exploration. With recent advances in technology, it is already possible to do a brute force on four bar search space as long as correct assumptions are made [10,11]. However even using aforementioned software it still takes quite a long time to finish the search (roughly 4 hours). There are also works on synthesizing function [12,13] but those studies are orthogonal to ours as their works focuses on making a connection between input angle and output angle while our works focuses on creating motion based on prescribed path. This work attempts to bridge the existing hole in the study by providing an algorithm that can produce four bar that is capable of producing the desired walking motion within more reasonable time limit.

After the design is finalized a prototype was fabricated using combination of additive (3D Printing) and traditional subtractive manufacturing. This is to ensure both the viability of the mechanism (no interference) and the validity of the claim mentioned previously (that a CNC machine is not necessary to produce the desired motion). While we still require the use of 3D printer to produce the body of the toy its use is less pronounced compared to previous works. 3D Printing has enjoyed quite immense popularity in the recent year mainly due to major patents expiring sometime in 2009 [10]. It works by depositing molten plastic on top of moving base layer by layer. It has been used for research in various fields such as microfluidics [15,16], optics [17,18], biomedicine [19], and even aerospace [20].

2 Design

First consider a four-bar linkage that reaches a limiting point at position 1 and 3 as shown in figure 1. In this text notation similar to that of Sandor-Erdman [21] will be used

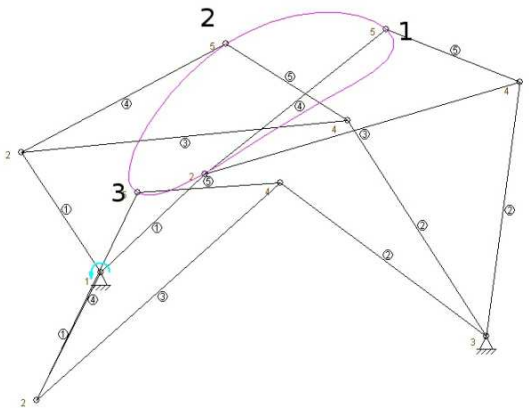

Figure 1 Four-bar Linkage with 2 Endpoints

A typical four-bar linkage design is typically done by splitting the linkages into two parts called dyads. Equations

Acta Mechatronica - International Scientific Journal about Mechatronics
Volume: 5 2020 Issue: 4 Pages: 53-60 ISSN 2453-7306

DESIGN AND FABRICATION OF RUNNING CHEETAH MECHANICAL TOY USING FOUR-BAR LINKAGE

Adimas Wicaksana

for both dyads can then be solved simultaneously. Let us initially consider the left dyad that contains the prime mover and ignore the right dyad as shown in figure 2.

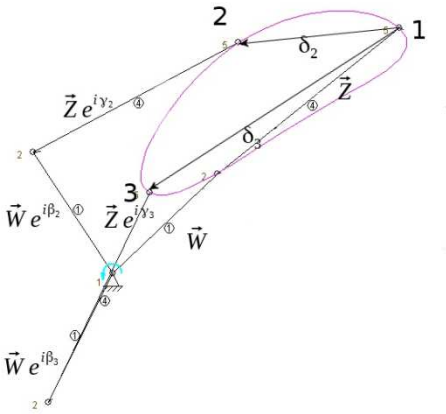

Figure 2 Left Dyad

From figure 2 we can see that the curves endpoints are reached when W and Z either points to the same direction or exact opposite of each other so we can get (1).

$$\vec{W} = a\vec{Z} \tag{1}$$

Where *a* is a scalar signifying the ratio of length of *Z* with respect to length of *W*.

Note that this is a sufficient but not necessary condition as there are cases where the endpoint is reached without W and Z pointing to the same direction or opposite to each other but as we can see in the case study later the search space for our method is wide enough that we won't need to consider all the possible cases (2).

$$\vec{\mathbf{W}}\left(\mathbf{e}^{\mathbf{i}\beta_3} - \mathbf{1}\right) + \vec{\mathbf{Z}}(\mathbf{e}^{\mathbf{i}\gamma_3} - \mathbf{1}) = \vec{\boldsymbol{\delta}}_3 \tag{2}$$

But we know that at position 3 W and Z points to opposite direction as compared to position 1 so we have (3).

$$\vec{W}\mathrm{e}^{\mathrm{i}\beta_3} = -a\vec{Z}\mathrm{e}^{\mathrm{i}\gamma_3} \tag{3}$$

Substituting Z from this equation (4) into (2)

$$\boldsymbol{W} = \frac{\vec{\boldsymbol{\delta}}_3}{\mathbf{e}^{\mathbf{i}\beta_3}(\mathbf{1}-\mathbf{a})-(\mathbf{1}+\mathbf{a})} \tag{4}$$

Similarly for position 2 we have (5)

$$\vec{\mathbf{W}}\left(\mathbf{e}^{\mathbf{i}\beta_2} - \mathbf{1}\right) + \vec{\mathbf{Z}}(\mathbf{e}^{\mathbf{i}\gamma_2} - \mathbf{1}) = \vec{\boldsymbol{\delta}}_2 \tag{5}$$

By substituting W and Z from (4) and (1) respectively we can get (6).

$$\frac{\vec{\boldsymbol{\delta}}_3}{\mathbf{e}^{\mathbf{i}\beta_3}(\mathbf{1}-\mathbf{a})-(\mathbf{1}+\mathbf{a})}\left(\mathbf{e}^{\mathbf{i}\beta_2} - \mathbf{1}\right) + \frac{\vec{\boldsymbol{\delta}}_3}{\mathbf{e}^{\mathbf{i}\beta_3}(\mathbf{1}-\mathbf{a})-(\mathbf{1}+\mathbf{a})}(\mathbf{e}^{\mathbf{i}\gamma_2} - \mathbf{1}) = \vec{\boldsymbol{\delta}}_2 \tag{6}$$

These are two equations (real and imaginary part) with 4 unknowns in β2, β3, γ2, and a. Since β2 and β3 are angles we can choose any number from 0 to 2π as our selections. Alternatively, if timings are important we can predetermine β2 and β3 since those angles correspond to crank angle for position 2 and 3. Either way for each pairs of β2, β3 we will have corresponding solutions in γ2 and a since each tuples must fulfil (6).

$$\begin{gathered}\mathbf{1} + \mathbf{2}\boldsymbol{a} + \boldsymbol{a}^{\mathbf{2}} - \mathbf{cos}(\boldsymbol{\beta}_2) - \mathbf{a}\,\mathbf{cos}(\boldsymbol{\beta}_2) - \mathbf{cos}(\boldsymbol{\beta}_3) \\ +\boldsymbol{a}^{\mathbf{2}}\,\mathbf{cos}(\boldsymbol{\beta}_3) + \mathbf{cos}(\boldsymbol{\beta}_2)\,\mathbf{cos}(\boldsymbol{\beta}_3) - \boldsymbol{a}\,\mathbf{cos}(\boldsymbol{\beta}_2)\,\mathbf{cos}(\boldsymbol{\beta}_3) \\ \mathbf{a}\,\mathbf{cos}(\boldsymbol{\gamma}_2) - \mathbf{a}^{\mathbf{2}}\,\mathbf{cos}(\boldsymbol{\gamma}_2) + \boldsymbol{a}\,\mathbf{cos}(\boldsymbol{\beta}_3)\,\mathbf{cos}(\boldsymbol{\gamma}_2) \\ -\mathbf{a}^{\mathbf{2}}\,\mathbf{cos}(\boldsymbol{\gamma}_2)\,\mathbf{cos}(\boldsymbol{\beta}_3) + \mathbf{sin}\,(\boldsymbol{\beta}_2)\,\mathbf{sin}(\boldsymbol{\beta}_3) - \\ \mathbf{a}\,\mathbf{sin}\,(\boldsymbol{\beta}_2)\,\mathbf{sin}(\boldsymbol{\beta}_3) + \boldsymbol{a}\,\mathbf{sin}(\boldsymbol{\beta}_3)\,\mathbf{cos}(\boldsymbol{\gamma}_2) \\ -\boldsymbol{a}^{\mathbf{2}}\,\mathbf{sin}(\boldsymbol{\beta}_3)\,\mathbf{cos}(\boldsymbol{\gamma}_2) \\ = \boldsymbol{Re}\left(\frac{\vec{\boldsymbol{\delta}}_2}{\vec{\boldsymbol{\delta}}_3}\right)(\mathbf{2}(\mathbf{1}+\boldsymbol{a}^{\mathbf{2}}) + (-\mathbf{1}+\boldsymbol{a}^{\mathbf{2}})\,\mathbf{cos}(\boldsymbol{\beta}_3))\end{gathered} \tag{7}$$

We can solve this equation (7) by replacing cos γ_2 with x and sin γ_2 with $\sqrt{(1-x^2)}$. By collecting all terms with x on one side and $\sqrt{(1-x^2)}$ on the other and squaring both sides we can get quadratic equation in x. We can then represent x in terms of a (8). Next, we take a look at the imaginary part of (6).

$$\begin{gathered}-\mathbf{sin}(\boldsymbol{\beta}_2) - \mathbf{a}\ \mathbf{sin}(\boldsymbol{\beta}_2) + \mathbf{cos}(\boldsymbol{\beta}_3)\,\mathbf{sin}(\boldsymbol{\beta}_2) \\ -\mathbf{a}\,\mathbf{cos}(\boldsymbol{\beta}_3)\,\mathbf{sin}(\boldsymbol{\beta}_2) + \mathbf{sin}\,(\boldsymbol{\beta}_3) - \boldsymbol{a}^{\mathbf{2}}\,\mathbf{sin}(\boldsymbol{\beta}_3) \\ -\mathbf{cos}(\boldsymbol{\beta}_2)\,\mathbf{sin}(\boldsymbol{\beta}_3) + \boldsymbol{a}\,\mathbf{cos}(\boldsymbol{\beta}_2)\,\mathbf{sin}(\boldsymbol{\beta}_3) \\ -\mathbf{a}\,\mathbf{cos}(\boldsymbol{\gamma}_2)\,\mathbf{sin}(\boldsymbol{\beta}_3) + \mathbf{a}^{\mathbf{2}}\,\mathbf{cos}(\boldsymbol{\gamma}_2)\,\mathbf{sin}(\boldsymbol{\beta}_3) \\ -\mathbf{a}\,\mathbf{sin}(\boldsymbol{\gamma}_2) - \mathbf{a}^{\mathbf{2}}\mathbf{sin}(\boldsymbol{\gamma}_2) + \mathbf{a}\,\mathbf{cos}(\boldsymbol{\beta}_3)\,\mathbf{sin}(\boldsymbol{\gamma}_2) \\ -\mathbf{a}^{\mathbf{2}}\,\mathbf{cos}(\boldsymbol{\beta}_3)\,\mathbf{sin}(\boldsymbol{\gamma}_2) \\ = \boldsymbol{Im}\left(\frac{\vec{\boldsymbol{\delta}}_2}{\vec{\boldsymbol{\delta}}_3}\right)(\mathbf{2}(\mathbf{1}+\boldsymbol{a}^{\mathbf{2}}) + (-\mathbf{1}+\boldsymbol{a}^{\mathbf{2}})\,\mathbf{cos}(\boldsymbol{\beta}_3))\end{gathered} \tag{8}$$

Since x is cos γ_2 and $\pm\sqrt{(1-x_2)}$ is sin γ_2 we can replace all terms that contains γ_2 with either of those terms. We can then substitute x value with representation found from (7). The resulting equation only contains one unknown which is a, which can then find by numerically solving for the polynomials. Note that not all a that is found is a valid solution since there is possibility that x >1, x<-1 or even x is imaginary. That is why we will need to double check the solutions found against (5).

Acta Mechatronica - International Scientific Journal about Mechatronics
Volume: 5 2020 Issue: 4 Pages: 53-60 ISSN 2453-7306

DESIGN AND FABRICATION OF RUNNING CHEETAH MECHANICAL TOY USING FOUR-BAR LINKAGE

Adimas Wicaksana

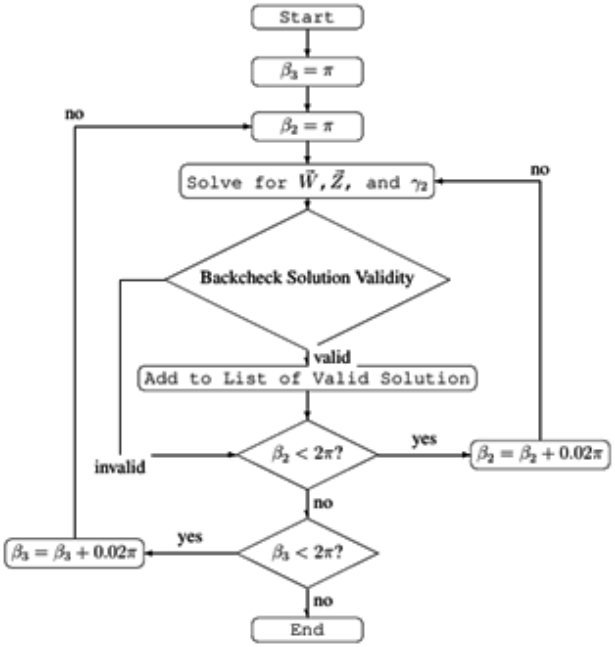

Figure 3 Left Dyad Design Procedure

Now let's take a look at the right dyad as depicted in figure 3.

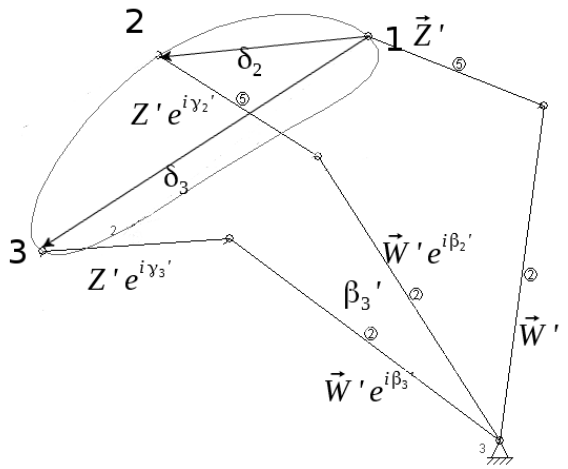

Figure 4 Right Dyad

Similarly the other dyad satisfy equation (2) and (5) as well (9).

$$\vec{\mathbf{W}}'\left(\mathbf{e}^{\mathbf{i}\beta_2'} - \mathbf{1}\right) + \vec{\mathbf{Z}}'(\mathbf{e}^{\mathbf{i}\gamma_2} - \mathbf{1}) = \vec{\boldsymbol{\delta}}_{\mathbf{2}} \qquad (9)$$

The prime symbol represents the counterpart for the right dyad. There is no prime symbol for $\gamma 2$ because the rotation angles are the same for both left and right dyad.

$$\vec{\mathbf{W}}'\left(\mathbf{e}^{\mathbf{i}\beta_3'} - \mathbf{1}\right) + \vec{\mathbf{Z}}'(\mathbf{e}^{\mathbf{i}\gamma_3} - \mathbf{1}) = \vec{\boldsymbol{\delta}}_{\mathbf{3}} \qquad (10)$$

So now we have four equations with 6 unknowns. Like the previous dyad we will iterate through both β2' and β3' from 0 to 2π. Likewise for each pairs we will generate its corresponding W' and Z'. Since (9) and (10) are linear equations in those two variables solving them should be pretty straightforward.

Once we have found the tuples (W, Z, W', Z') we have practically defined the four-bar linkage. We can then determine the suitability of the said linkage by considering the following:

1. Grashof Criterion.

Grashof criterion says that the sum of the longest link and the shortest link should be less than the sum of two remaining links. We can find the length of each links by taking the magnitude of vectors **W**, **W**, (**Z-Z'**), and (**W+Z-W'-Z'**) respectively.

2. Crank-rocker or Drag link configuration.

For a fourbar to make a complete rotation the shortest link needs to be either the ground or the input link. In other words among the four linkages either **W** or **W+Z-W'-Z'** needs to be the smallest of the four.

3. None of the coupler angles are imaginary.

We find every coupler angles for each input angle rotation that we are interested in using forward kinematics and verify that none of them are imaginary to make sure that we have a valid linkage.

4. Attempt to minimize the distance between each coupler positions and the supposed position.

We can do this by choosing angle combinations β_2, β_3, β_2', β_3' where the (11) reaches minimum.

$$\sum(\mathbf{P}_{\mathbf{x}_{\mathbf{design}}} - \mathbf{P}_{\mathbf{x}_{\mathbf{ideal}}})^2 + \sum(\mathbf{P}_{\mathbf{y}_{\mathbf{design}}} - \mathbf{P}_{\mathbf{y}_{\mathbf{ideal}}})^2 \qquad (11)$$

DESIGN AND FABRICATION OF RUNNING CHEETAH MECHANICAL TOY USING FOUR-BAR LINKAGE
Adimas Wicaksana

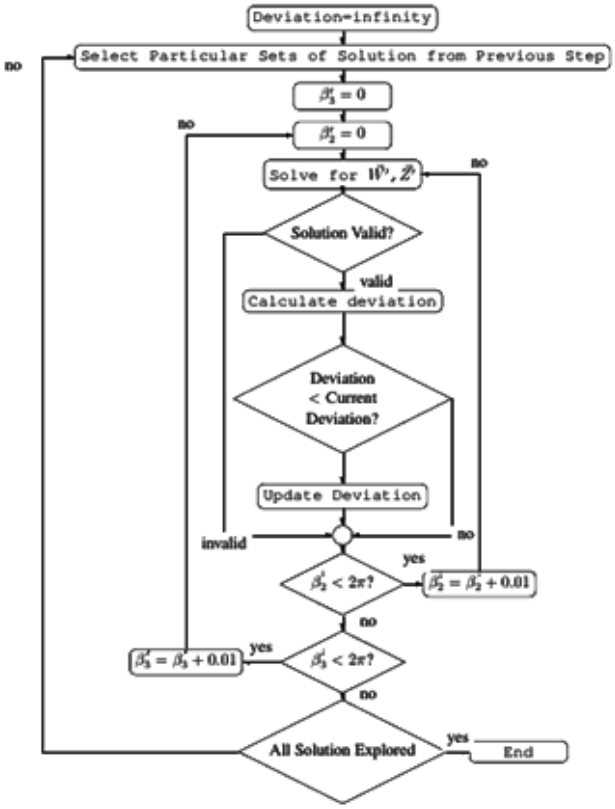

Figure 5 Right Dyad Design Procedure

3 Fabrication

First an animated image [22] was downloaded from the Internet to be used as a reference. For manufacturing simplicity, it is assumed that both left leg and right leg follows the same motion. The position of foreleg and hind leg at each frame is recorded in table 1. The leftmost and rightmost positions are selected as position 1 and 3 respectively. The positions where legs touch the ground is selected as position 2. We can then apply the calculation described in previous sections to the problem.

Ideally, we would like it so that each frame has similar spacing in β however attempting to pose this constraint tend to lead to unacceptable error in positions. As such the bottom part of the movement is time-stretched so that the error in positions can be minimized. Design for left dyad is implemented using Mathematica while the one for right dyad is implemented using Matlab. The linkage obtained is then simulated using software Artas SAM.

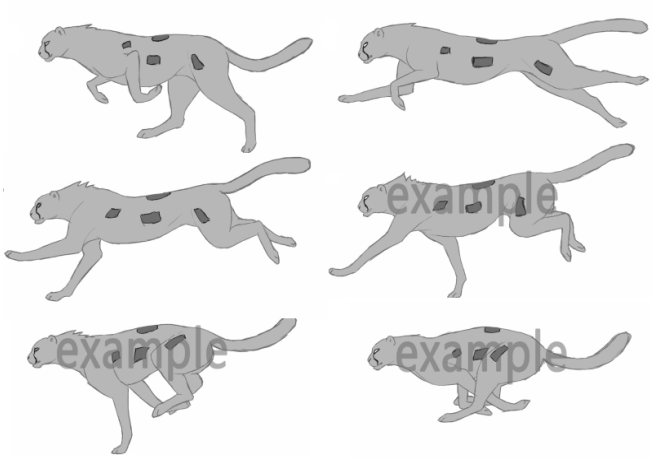

Figure 6 Reference Animation [22]

Table 1 Paw Positions in Pixel

Fore Leg (x)	Fore Leg (y)	Hind Leg (x)	Hind Leg (y)
0	32	125	44
8	31	165	12
63	0	297	3
149	3	343	24
215	56	381	43
231	68	391	91
197	66	377	90
187	79	341	58
143	63	340	62
96	60	294	48
51	63	244	48
11	69	197	50
13	66	149	62

After the design has been finalized each linkage was fabricated using combination of additive and subtractive manufacturing with conversion factor of 20 pixels/cm. Note that additive manufacturing process is not strictly required in the fabrication of the linkage. It is only used to shorten the waiting time while waiting for the raw material (acrylic) to arrive and to give good contrast whenever it is necessary. At the end of each linkage either a 3D-printed pin or a bearing was placed. For linkages made from acrylic the pin was connected by welding the pin into the acrylic using soldering iron. For linkages that are 3D-printed the pins are printed at the same time as the linkage. Bearings were placed by pushing them into the hole made either by drilling (for acrylic) or pre-made hole during printing (for 3D-printed part). The body of the toy was

DESIGN AND FABRICATION OF RUNNING CHEETAH MECHANICAL TOY USING FOUR-BAR LINKAGE
Adimas Wicaksana

made by 3D-printing the part as well. Similarly, a bearing was also placed inside the body of the toy.

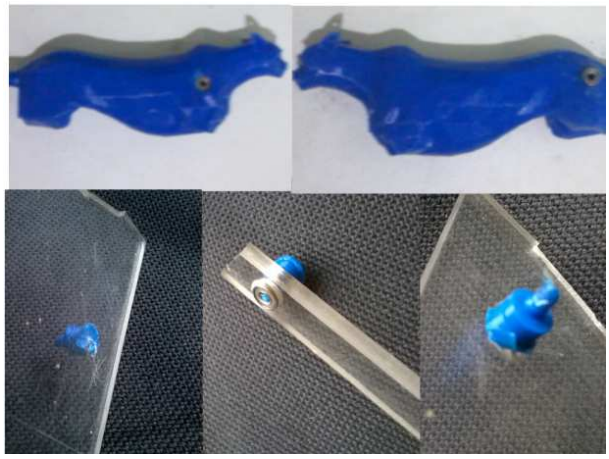

Figure 7 Revolute Joints

4 Results and Discussion

Figure 8 shows the linkage generated from our procedure that is to be connected to foreleg.

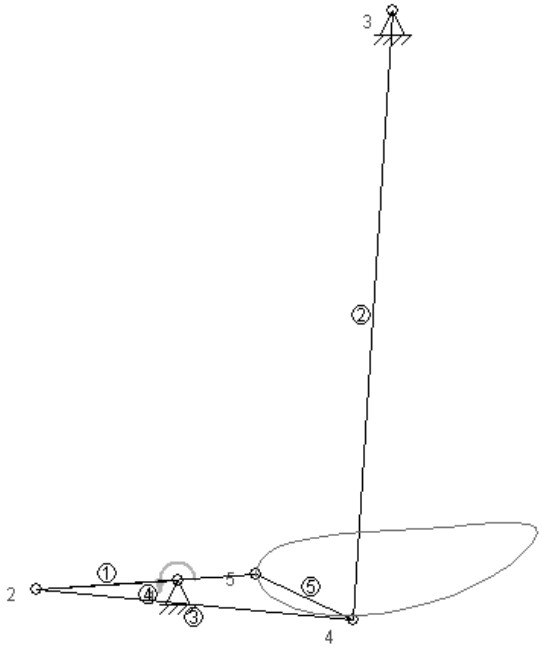

Figure 8 Front Leg Linkage

The crank has dimension of 5.8 cm, the rocker has dimension of 25 cm, the coupler has sides with dimensions of 4 cm, 9 cm, and 13 cm respectively. Meanwhile the frame (distance between pivots) is 25 cm long. We can still 3D-print the crank and the coupler while we need to use acrylic for the rocker since it is much larger than maximum size that Lulzbot can print. Meanwhile table 2 shows comparison between x and y generated by the linkage and the one from reference animation.

Table 2 Comparison between x and y positions of front leg

X Actual	X Reference	Y Actual	Y Reference
0.000	0.000	32.000	32.000
19.004	8.000	9.405	31.000
71.085	63.000	-2.191	0.000
142.769	149.000	8.352	3.000
206.101	215.000	38.736	56.000
230.999	231.000	68.000	68.000
217.926	197.000	74.837	66.000
183.068	187.000	73.392	79.000
135.030	143.000	69.378	63.000
87.450	96.000	66.336	60.000
48.860	51.000	62.653	63.000
21.311	11.000	55.885	69.000
4.908	13.000	45.348	66.000

As can be seen from table above the for the key frames (points 1, 2, and 3 during the design) are exact, meaning that the reference and actual positions as reached by the linkage are the same. By inserting these values into (11) we can get the squared-sum of position errors to be 2658 pixels, which corresponds to root-mean-square of 14.3 pixels, which are significantly smaller than the perimeter of the traced path (531 as measured by Autocad).

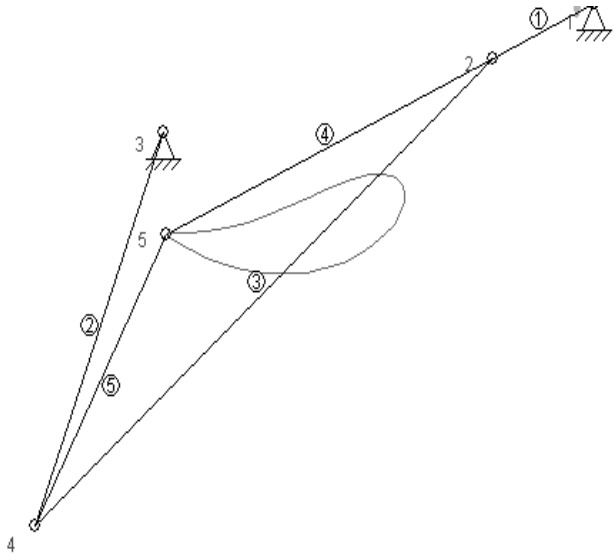

Figure 9 Hind Leg Linkage

The linkage for hind leg has crank with dimension of 6.3 cm, rocker with dimension of 20 cm, and coupler with sides of 34 cm, 20 cm, and 16 cm respectively. Distance between pivots is 25 cm long as well. Similarly, we can use 3D printer to produce the crank while the rocker and the coupler need to be made from acrylic.

DESIGN AND FABRICATION OF RUNNING CHEETAH MECHANICAL TOY USING FOUR-BAR LINKAGE
Adimas Wicaksana

Table 3 Comparison between x and y positions of hind leg

X Actual	X Reference	Y Actual	Y Reference
125.000	125.000	44.000	44.000
168.252	165.000	22.006	12.000
253.796	297.000	5.823	3.000
336.620	343.000	21.804	24.000
385.628	381.000	60.057	43.000
388.612	391.000	93.969	91.000
372.658	377.000	101.852	90.000
346.575	341.000	100.261	58.000
311.844	340.000	89.674	62.000
269.554	294.000	73.067	48.000
221.436	244.000	56.245	48.000
173.050	197.000	46.312	50.000
136.671	149.000	45.172	62.000

Similarly, for key frames the actual and reference positions are the same. Plugging these values into (11) will result in squared-sum of position error of 8718, which correspond to root-mean square of 25.9 pixels, which are much smaller than the perimeter of 616 as measured by Autocad.

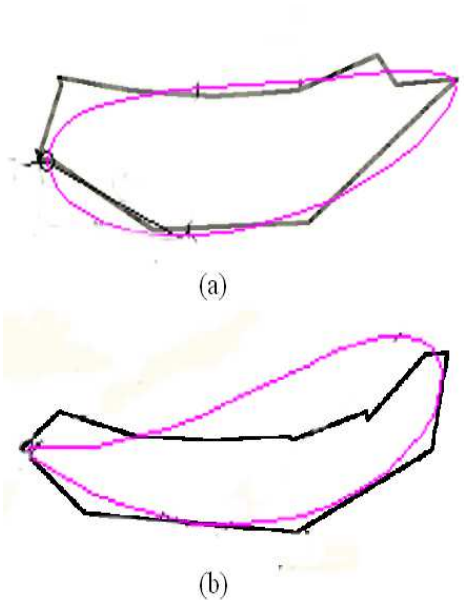

Figure 10 Visual Representation of Linkage Movement, Actual(pink) vs Reference(black), for front leg (a) and hind leg (b)

Figure 10 shows visual representation of these values so that we can evaluate the performance of the linkage qualitatively.

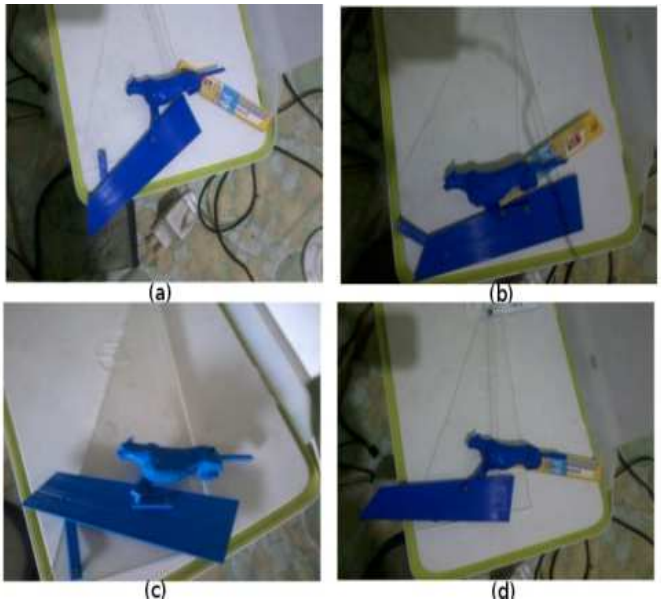

Figure 11 front leg mechanism at bottom-most (a), right-most (b), top-most(c), and left-most positions(d)

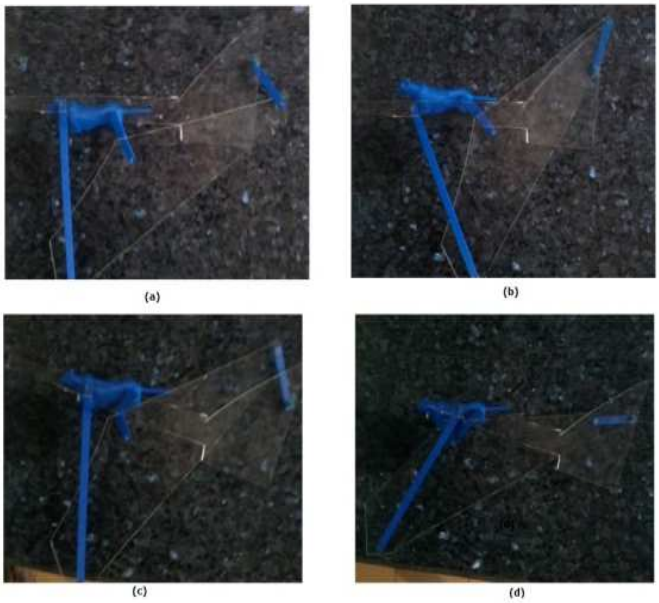

Figure 12 Fabricated mechanism at bottom-most (a), right-most (b), top-most(c), and left-most(d) positions

Prior to his work there have been several works that related to generating specific path for animation or motion capture purpose. Ceylan and Thomaszewski made some study regarding mechanism as internal part of the toy [3,4]. While their works are more elegant than ours it comes at a price of more complex assembly and manufacture. . In particular Ceylan's work requires the use of laser cutter and Thomaszewski's work requires 11 separate links compared to 5 links described in this paper. Our work is closer to the original work by Zu and Coros where the movers are completely separate from the toy [1,2]. While the problem

is much simpler because it poses less constraints both of their work still requires more extensive manufacturing process where it requires either cam or gears inside the mechanism. In contrast four-bar linkage only uses a rigid link which is relatively simpler to manufacture because unlike gears or cam producing a rigid link only requires motion in single axis as compared to two or more for gears or cam.

5 Conclusion

Method to design four bar linkage based on its endpoints and a specified path has been presented. This method has been applied to generate a motion on a running cheetah toy. The designed mechanism was subsequently fabricated using traditional manufacturing method (no CNC) to demonstrate its manufacturing viability. Motion generated by the mechanism has relatively small error (less than 10x) compared to the total perimeter of the traced path. The linkage generated is also the simplest of all previous work. The procedure discussed in the text can also be applied to design pick-and-place mechanism where the workspace is constrained. Since the procedure actually take into account the limiting position of the coupler curve we can tell its endpoint quite easily.

References

[1] ZHU, L., XU, W., SNYDER, J., LIU, Y., WANG, G., GUO, B.: Motion-Guided Mechanical Toy Modeling, *ACM Transactions on Graphics*, Vol. 31, No. 6, pp. 1-10, 2012.

[2] COROS, S., THOMASZEWSKI, B., NORIS, G., SUEDA, S., FORBERG, M., SUMMER, R.W., MATUSIK, W., BICKEL, B.: Computational Design of Mechanical Characters, *ACM Transactions on Graphics*, Vol. 32, No. 4, pp. 1-12, 2013.

[3] THOMASZEWSKI, B., COROS, S., GAUGE, D., MEGARO, V., GRINSPUN, E., GROSS, M.: Computational Design of Linkage-Based Characters, *ACM Transactions on Graphics*, Vol. 33, No. 4, pp. 1-9, 2014.

[4] CEYLAN, D., LI, W., MITRA, N.J., AGRAWAKA, M., PAULY, M.: Designing and Fabricating Mechanical Automata from Mocap Sequences, *ACM Transactions on Graphics*, Vol. 32, No. 6, pp. 1-11, 2013.

[5] SLEESONGSOM, S., BUREERAT, S.: Four-Bar Linkage Path Generation through Self-Adaptive Population Size Teaching-Learning Based Optimization, *Knowledge-Based Systems*, Vol. 135, pp. 180-191, 2017.

[6] KIM, J.W., SEO, T., KIM, J.: A new design methodology for four-bar linkage mechanisms based on derivations of coupler curve, *Mechanism and Machine Theory*, Vol. 100, pp. 138-154, 2016.

[7] ZBIKOWSKI, R., GALINSKI, C., PEDERSEN, C.B.: Four-Bar Linkage Mechanism for Insect-like Flapping Wings in Hover: Concept and an Outline of Its Realization, *Journal of Mechanical Design*, Vol. 127, pp. 817-824, 2005.

[8] SINGH, R., CHAUDHARY, H., SINGH, A.K.: Defect-free optimal synthesis of crank-rocker linkage using nature-inspired optimization algorithms, *Mechanism and Machine Theory*, Vol. 116, pp. 105-122, 2017.

[9] ACHARYYA, S., MANDAL, M.: Performance of EAs for Four Bar Linkage Synthesis, *Mechanism and Machine Theory*, Vol. 44, pp. 1784-1794, 2009.

[10] HAUENSTEIN, J.D., SOTTILE, F.: Algorithm 921: AlphaCertified: Certifying Solutions to Polynomial Systems, *ACM Transansction on Mathematical Software*, Vol. 38, No. 4, pp. 1-20, 2012.

[11] WAMPLER, C., MORGAN, A., SOMMESE, A.: Complete solution of the Nine Point Path Synthesis Problem for Four-Bar-Linkages, *Transaction of the ASME*, Vol. 114, pp. 153–159, 1992

[12] LI, X., WEI, S., LIAO, Q., ZHANG, Y.: A Novel Analytical Method for Function Generation Synthesis of Planar Four-Bar Linkage, *Mechanism and Machine Theory 101*, Vol. 101, pp. 222–235, 2016

[13] FREUDENSTEIN, F.: Approximate Synthesis of Four-Bar Linkages, *Resonance*, Vol. 15, pp. 740-767, 2010.

[14] WAHEED, S., CABOT, J.M., MacDONALD, N.P., LEWIS, T., ROSANNE, M.G., PAULL, B., BREADMORE, M.C.: 3D printed microfluidic devices: enablers and barriers, *Lab on a Chip*, Vol. 16, pp. 1993-2013, 2016.

[15] HO, C.M.B., NG, S.H., LI, K.H.H.J., YOON, Y.: 3D printed microfluidics for biological applications, *Lab on Chip*, Vol. 15, No. 18, pp. 3627-3637, 2015.

[16] GONG, H., BICKHAM, B.P., WOOLLEY, A.T., NORDIN, G.P.: Custom 3D printer and resin for 18 μm × 20 μm microfluidic flow channels, *Lab on a Chip*, Vol. 17, No. 17, pp. 2899-2909, 2017.

[17] BUSCH, S.F., WEIDENBACH, M., FEY, M., SCHÄFER, F., PROBST, T., KOCH, M.: Optical Properties of 3D Printable Plastics in the THz Regime and their Application for 3D Printed THz Optics, *Journal of Infrared, Millimeter, and Terahertz Waves*, Vol. 35, No. 12, pp. 993-997, 2014.

[18] BUSCH, S.F., WEIDENBACH, M., BALZER, J.C., KOCH, M.: THz Optics 3D Printed with TOPAS, *Journal of Infrared, Millimeter, and Terahertz Waves*, Vol. 37, No. 4, pp. 303-307, 2016.

[19] INZANA, J.A., OLVERA, D., FULLER, S.M., KELLY, J.P., GRAEVE, O.A., SCHWARZ, E.M., KATES, S.L., AWAD, H.A.: 3D printing of composite calcium phosphate and collagen scaffolds for bone regeneration, *Biomaterials*, Vol. 35, No. 13, pp. 4026-4034, 2014.

[20] JOSHI, S.C., SHEIKH, A.A.: 3D printing in aerospace and its long-term sustainability, *Virtual*

and Physical Prototyping, Vol. 10, No. 4, pp. 175-185, 2015.

[21] SANDOR, G., ERDMAN, A.: *Advanced Mechanism Design: Analysis and Synthesis*, Vol. II, Englewood Cliffs, John Wiley and Sons, 1984.

[22] NORTHERNRED: Cheetah running cycle frames + PSD, [Online], Available: https://www.deviantart.com/northernred/art/Cheetah-running-cycle-frames-PSD-585490902 [20 Feb 2018], 2018.